



# Numerical Investigation of Obstacle Orientation–Induced Mixing Enhancement in Passive Micromixers



Hajar Moghadas\*

Department of Mechanical Engineering, Yasouj University, 74934-75918 Yasouj, Iran

\* Correspondence: Hajar Moghadas (h.moghadas@yu.ac.ir)

**Received:** 04-05-2026**Revised:** 05-28-2026**Accepted:** 06-13-2026

**Citation:** H. Moghadas, “Numerical investigation of obstacle orientation–induced mixing enhancement in passive micromixers,” *Power Eng. Eng. Thermophys.*, vol. 5, no. 3, pp. 193–201, 2026. <https://doi.org/10.56578/peet050301>.



© 2026 by the author(s). Licensee Acadlore Publishing Services Limited, Hong Kong. This article can be downloaded for free, and reused and quoted with a citation of the original published version, under the CC BY 4.0 license.

**Abstract:** Efficient mixing under laminar flow conditions remains a critical challenge in microfluidic systems because molecular diffusion alone is generally insufficient to achieve rapid and homogeneous species transport. In this study, the influence of obstacle orientation on mixing performance in passive micromixers was systematically investigated through numerical simulations. Inclined straight obstacles with orientation angles of 15°, 30°, 45°, and 60° were incorporated into microchannels under both leaky and leak-free configurations. Flow and concentration fields were solved using COMSOL Multiphysics, and the resulting mixing efficiencies and times were quantitatively evaluated. It was found that the introduction of inclined obstacles substantially enhanced mixing performance relative to a simple unobstructed microchannel. Superior mixing behavior was consistently achieved in the leak-free configuration, where stronger flow perturbations and more pronounced recirculation zones were generated within the central mixing region. For the leak-free configuration, mixing efficiency was observed to increase with decreasing obstacle angle. In contrast, no monotonic relationship between obstacle angle and mixing performance was identified for the leaky configuration. Among all investigated designs, the 15° obstacle configuration exhibited the highest overall performance, achieving mixing efficiencies of approximately 92% and nearly 100% in the leaky and leak-free configurations, respectively. To further evaluate the influence of geometric scale, the microchannel length was doubled for the 45° configuration. Enhanced concentration uniformity and reduced mixing time were achieved in the extended leaky microchannel, whereas no improvements were observed in the corresponding leak-free design. These findings demonstrate that obstacle orientation and channel configuration exert a strong influence on microscale transport phenomena and mixing enhancement. The proposed obstacle-based passive micromixer design provides an effective and energy-efficient strategy for improving mixing performance in microfluidic devices and offers valuable design guidelines for applications in biomedical analysis, chemical processing, and lab-on-a-chip systems.

**Keywords:** Passive micromixer; Microchannel flow; Mixing enhancement; Mass transfer; Numerical simulation; Obstacle orientation; Flow characteristics

## 1 Introduction

Micromixers are essential microfluidic devices designed to promote rapid and homogeneous mixing of fluids at the microscale [1, 2]. Owing to their compact structure and high transport efficiency, micromixers have attracted considerable attention in biomedical engineering, chemical synthesis, pharmaceutical processing, and microscale transport systems [3–6]. They have been widely employed in applications such as nanoparticle synthesis [7–9], biomarker detection [10, 11], and controlled mixing of multiple fluid streams in microfluidic platforms [12, 13]. Because of the small characteristic dimensions of microchannels, fluid flow inside micromixers is generally dominated by laminar behavior with low Reynolds numbers [14–16]. Under such conditions, viscous forces suppress transverse fluid motion, and molecular diffusion becomes the primary mixing mechanism, resulting in relatively slow mixing rates [17]. Improving mixing performance under laminar flow conditions therefore remains a major challenge in microfluidic systems.

To enhance mixing efficiency, both active and passive micromixing strategies have been developed [18, 19]. Active micromixers rely on external energy sources, including magnetic fields [20], electric fields [21], and acoustic excitation [22], to generate flow perturbations and improve species transport. In contrast, passive micromixers utilize

geometric modifications within the microchannel to manipulate flow behavior without external energy input [23]. Various passive designs have been proposed, including embedded obstacles, baffles, curved channels, and complex flow paths, which promote mixing by inducing secondary flow structures and localized vortices. Previous studies have demonstrated that the geometric configuration of obstacles significantly influences the hydrodynamic characteristics and mixing performance of microchannels [24, 25].

Despite their effectiveness, many reported passive micromixers involve highly complicated geometries that increase fabrication difficulty and manufacturing cost. Examples include displaced herringbone structures [26], rhombic barriers [27], and fractal-shaped stepped obstacles [28]. Although these configurations can improve mixing performance, their structural complexity limits practical implementation and large-scale fabrication [29–31]. Therefore, the development of simple and efficient passive micromixer designs remains an important research objective.

Jain and Unni [32] introduced a passive micromixer incorporating inclined blade obstacles positioned at a 45° angle relative to the transverse direction of the microchannel. Two configurations were considered, namely leak-free and leaky arrangements. The results showed that the leak-free design achieved a mixing efficiency of 88%, while the leaky configuration reached 82% in a 190 μm long microchannel. Since obstacle geometry strongly affects microscale flow characteristics and species transport, further investigation of obstacle orientation is required to better understand its influence on mixing enhancement. Accordingly, the present study numerically investigates the effect of obstacle inclination angle on the mixing behavior of passive micromixers using both leak-free and leaky configurations. Obstacle angles of 15°, 30°, 45°, and 60° are examined and compared in terms of concentration distribution, mixing efficiency, and mixing time. In addition, the influence of microchannel length on the mixing performance of the 45° configuration is evaluated. The objective is to identify a simple geometric configuration capable of improving mixing performance while maintaining structural simplicity and fabrication feasibility.

## 2 Methods

In this study, the performances of a simple micromixer and micromixers equipped with barriers at different angles of 15°, 30°, 45°, and 60° were compared. The analysis involved two designs: a leaky configuration and a leak-free configuration. Figure 1 illustrates both the simple micromixer and the micromixer featuring 15° blades, positioned relative to the middle axis of the channel under both leaky and leak-free designs. As shown in the figure, Fluid 1 and Fluid 2 enter from different inlets with different concentrations and then they are mixed at the horizontal part of the microchannel.

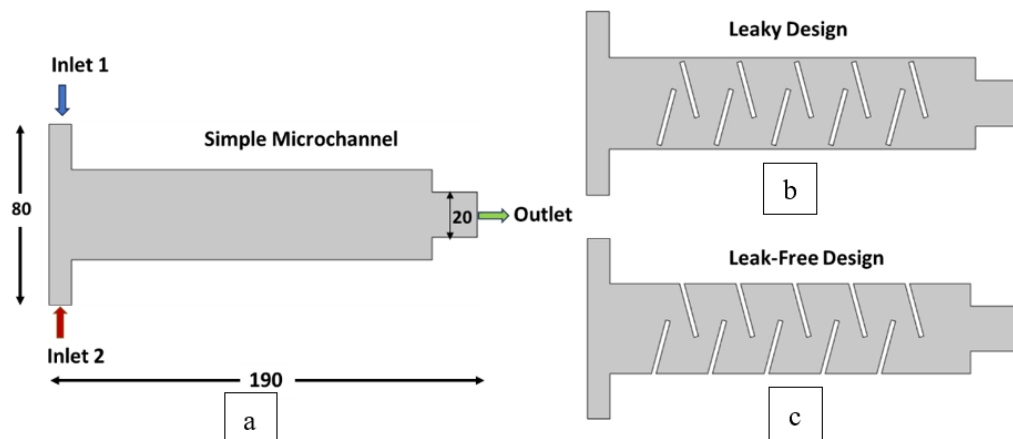


**Figure 1.** Micromixer designs: (a) simple; (b) leaky with 15° blades; and (c) leak-free with 15° blades

All steps involved in geometry generation, meshing, and flow solution were carried out using COMSOL Multiphysics (Version 6.2). The meshing process utilized irregular triangular elements. To ensure that the solution was independent of the mesh count, velocity and concentration values were measured at five random points with progressively finer meshes. A mesh with an error of less than 1% was chosen as optimal. For the leaky mixer with 15° blades, the selected mesh consisted of 14,946 elements. Figure 2 illustrates an example of the mesh created for a mixer without leakage, featuring 15° blades.

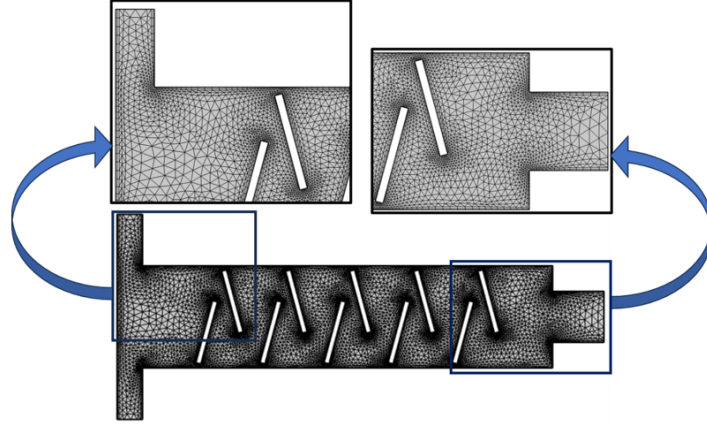


**Figure 2.** Computational mesh and enlarged view of the blade–wall region

## 2.1 Governing Equations and Boundary Conditions

This study used the governing equations for the continuity equation, Navier–Stokes, and the concentration equation as follows [32]:

$$\nabla \cdot \mathbf{V} = 0 \quad (1)$$

$$\rho \frac{\partial \mathbf{V}}{\partial t} + \rho(\mathbf{V} \cdot \nabla)\mathbf{V} = -\nabla p + \mu \nabla^2 \mathbf{V} + \mathbf{F} \quad (2)$$

$$\frac{\partial c}{\partial t} + (\mathbf{V} \cdot \nabla)c = D \nabla^2 c \quad (3)$$

where,  $\mathbf{V}$  represents the fluid velocity vector;  $\rho$  denotes the fluid density;  $p$  is the pressure;  $\mu$  indicates the dynamic viscosity of the fluid;  $\mathbf{F}$  denotes the volumetric forces per unit volume;  $c$  is the concentration; and  $D$  is the diffusion coefficient.

The no-slip condition was applied to all walls. Inlets 1 and 2 were subject to an inlet flow boundary condition with a velocity ranging from  $4 \times 10^{-4}$  m/s, while an outlet flow boundary condition was applied at the outlet. Fluid 1 was introduced at a concentration of  $1 \text{ mol/m}^3$ , and Fluid 2 was pure solvent at a concentration of  $0 \text{ mol/m}^3$ . The density was set at  $\rho = 1000 \text{ kg/m}^3$ , the dynamic viscosity was  $\mu = 0.001 \text{ Pa}\cdot\text{s}$ , and the diffusion coefficient was  $D = 1 \times 10^{-10} \text{ m}^2/\text{s}$  [32].

The comparison of different designs was based on the difference between the highest and lowest concentration values at the outlet as follows:

$$\varepsilon = c_{\max} - c_{\min} \quad (4)$$

where,  $\varepsilon$  denotes the concentration difference, or concentration non-uniformity, between the maximum and minimum outlet concentrations. The optimum condition was  $\varepsilon = 0$ , which was the state for maximum mixing.

The efficiency of the mixer ( $\eta_{\text{mix}}$ ) was defined as follows:

$$\eta_{\text{mix}} = \frac{0.5 - \varepsilon}{0.5} \times 100 \quad (5)$$

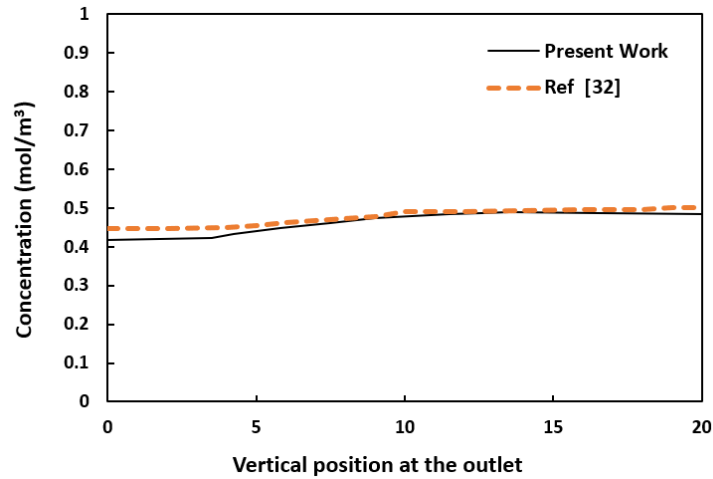
The value of 0.5 in that formula was the highest possible concentration of the mixture.

## 3 Results

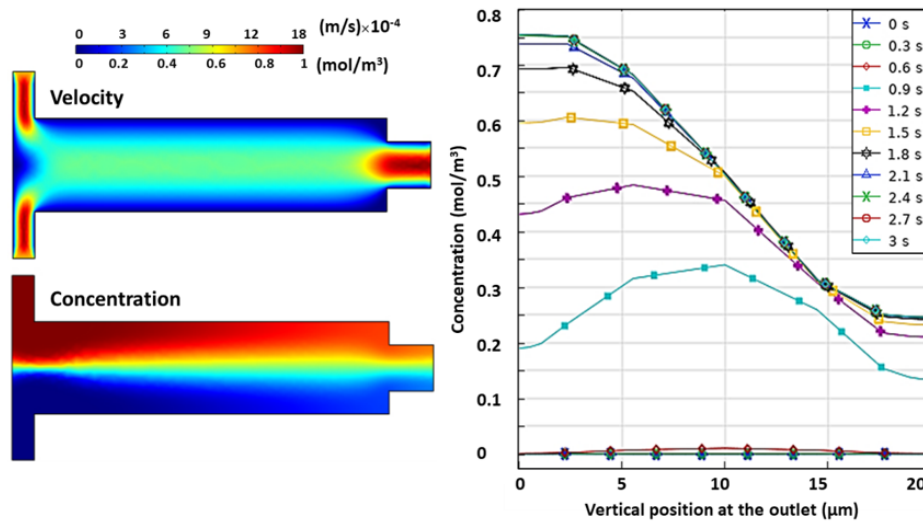
In the present study, different designs of leaky and leak-free micromixers with and without barriers were simulated with different lengths and angles. Firstly, the  $45^\circ$  sample that was previously investigated by Jain and Unni [32] was simulated for validation in the present study. As shown in Figure 3, the concentration distribution results obtained in the present work exhibited good agreement with the results obtained by Jain and Unni [32].

Figure 4 illustrates the velocity contour, concentration distribution, and concentration graph at the outlet of a simple micromixer. The velocity contour showed that, due to the very low velocity, the flow reached a fully developed state within a short distance inside the microchannels. Meanwhile, the concentration distribution contour indicated

minimal mixing at the interface between the two fluids. The data presented demonstrates that after two seconds, the concentration distribution at the outlet stabilized. Under these conditions, the difference between the maximum and minimum concentrations at the outlet was 0.5, and the concentration graph exhibited a steep slope, indicating inhomogeneous and undesirable mixing. That was the reason that prompted researchers to explore methods to enhance the performance of micromixers.



**Figure 3.** Comparison of concentration distributions at the micromixer outlet with the 45° barriers between the present work and Ref. [32]



**Figure 4.** Velocity contour, concentration distribution, and concentration diagram at the outlet of a simple micromixer

Figure 5 and Figure 6 show the velocity contour and concentration distribution inside the microchip, along with the concentration diagrams at the outlet for the leaky and leak-free micromixers at different obstacle angles, respectively. In the leaky design, the highest local velocity occurred in the central areas near the obstacles. The best mixing performance was achieved at an angle of 15°, which exhibited a relatively uniform green distribution at its outlet region, corresponding to an optimal concentration of 0.5. The outlet concentration distributions yielded  $\epsilon$  values of 0.05, 0.18, 0.09, and 0.17 for obstacle angles of 15°, 30°, 45°, and 60°, respectively. Thus, in the leaky case, the angle of 15° achieved the best performance, followed by 45°. The slope of the concentration line at the outlet for the 15° angle was very gentle, indicating a uniform concentration after mixing. The design featuring the 15° angle achieved a relatively stable concentration with an efficiency of 92% after 2 seconds, while the 45° sample reached an efficiency of 82% after 3 seconds. Here, the difference between the maximum and minimum mixing rates at the output was influenced by the angle of the obstacles; however, this relationship did not follow a proportional trend of either increase or decrease.

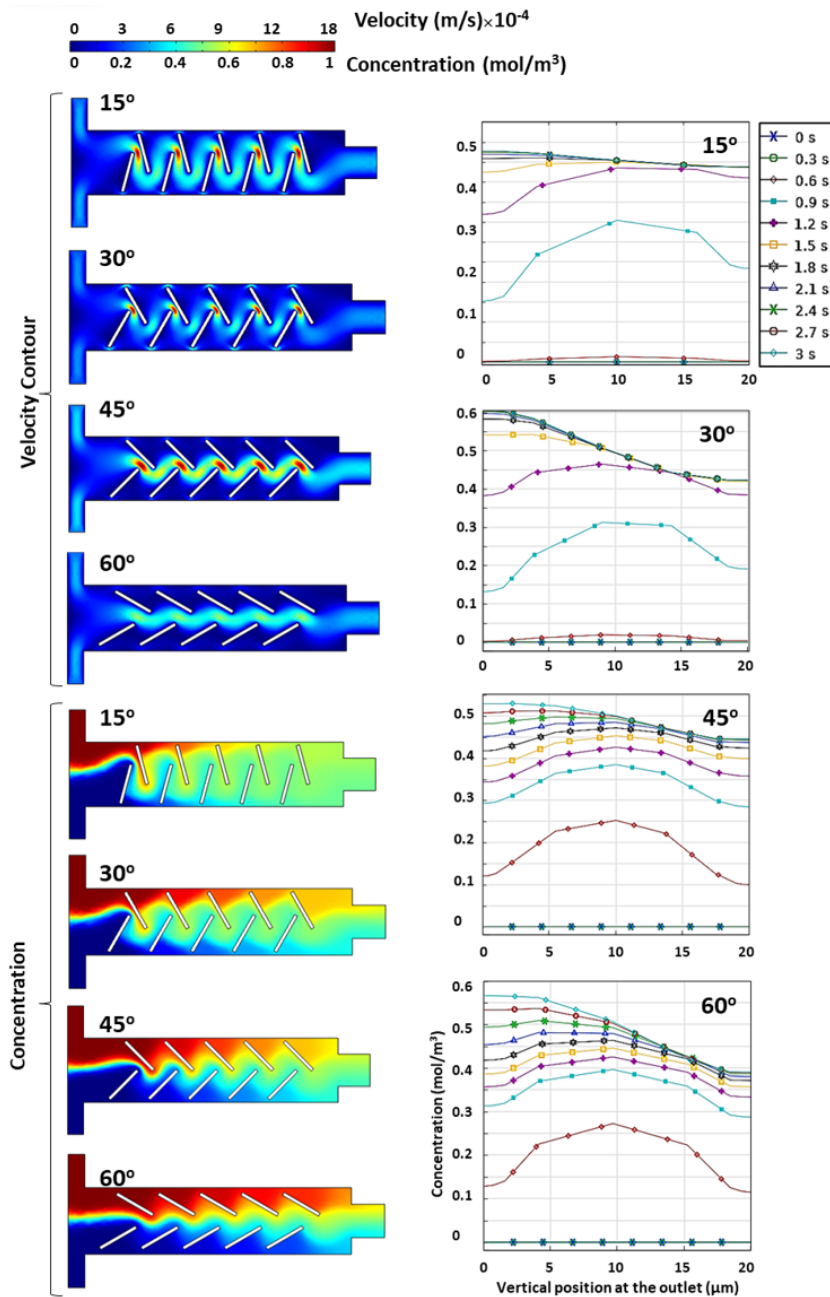


**Figure 5.** Velocity contours, concentration distributions, and outlet concentration profiles for the leaky micromixer at obstacle angles of 15°, 30°, 45°, and 60°

The leak-free samples exhibited a similar velocity distribution to the leaky samples, but with noticeable differences: stronger velocity contours were seen in the central areas of the microchannel for the leak-free samples. An examination of the concentration distribution across different designs revealed that all the leak-free samples demonstrate better mixing compared to their leaky counterparts. That improved mixing can be attributed to the increased flow rate in the central regions of the leak-free microchannel, which generated more pronounced vortices, thereby enhancing the mixing process. In the leak-free samples with 15° and 30° designs, a relatively uniform green concentration, indicative of complete mixing, was observed starting from the middle of the microchannel. These two samples recorded a mixing efficiency of approximately 100% at the outlet within less than 2 seconds, as shown in Figure 6. The slope of the concentration line at the outlet was nearly zero, signifying homogeneous and uniform mixing. For the design with a 45° angle, the mixing efficiency was about 88%, revealed by a gentle slope and a relatively uniform concentration distribution. A comparison of the leak-free samples with obstacle angles of 15° and 30° revealed nearly identical mixing efficiencies approaching 100%, which were achieved over the shortest mixing distance and within the shortest mixing time. In the leak-free samples, the difference between the maximum and

minimum mixing rates at the micromixer outlet diminished proportionally with an increase in the angle. Table 1 shows the mixing efficiency for the leaky and leak-free micromixers at different obstacle angles.

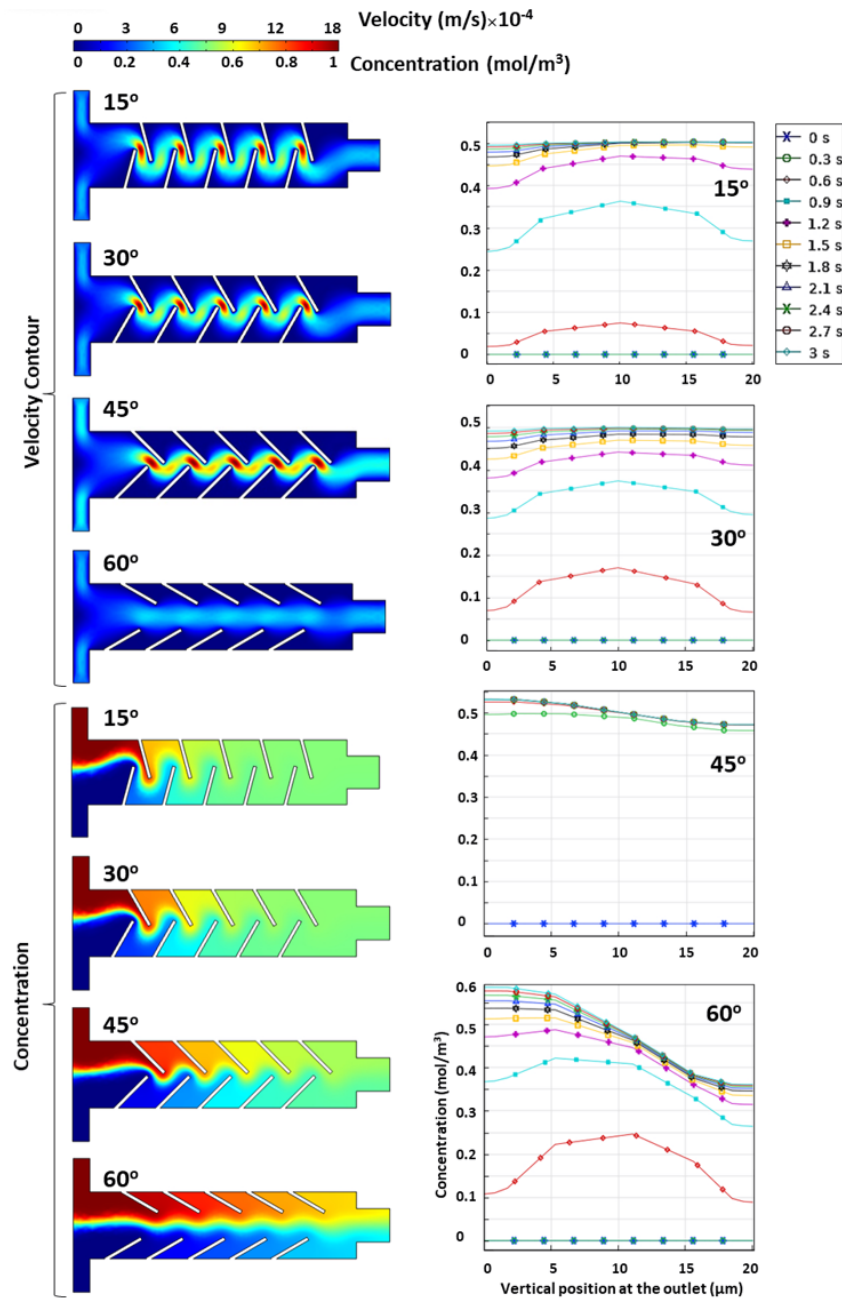


**Figure 6.** Velocity contours, concentration distributions, and outlet concentration profiles for the leak-free micromixer at obstacle angles of 15°, 30°, 45°, and 60°

**Table 1.** Mixing efficiency and mixing time for leaky and leak-free micromixers at different obstacle angles

Obstacle Angles	Leaky		Leak-Free	
	Mixing Efficiency (%)	Mixing Time (s)	Mixing Efficiency (%)	Mixing Time (s)
15°	92	2.1	99	3
30°	64	2.4	92	3
45°	82	3	88	0.9
60°	66	3	54	3

In the present study, the effect of increasing the length of the mixing microchannel in the 45° sample was also investigated. Figure 7 shows the results of increasing the length of the microchannel in the 45° sample for both leaky and leak-free samples. Analyzing the concentration results from the outlet indicated that the performance of the leak-free sample exceeded that of the leaky design, as previously observed in the other cases. In this situation for the leak-free design, the mixing efficiency became approximately 100% just after 0.9 seconds. However, no improvement in the mixing of the leaky design was observed with the increased length of the microchannel. In the leaky 45° design, the mixing time was 6 seconds. These findings indicate that while extending the length of the microchannel enhances mixing, the time required for complete mixing varies across different geometries.

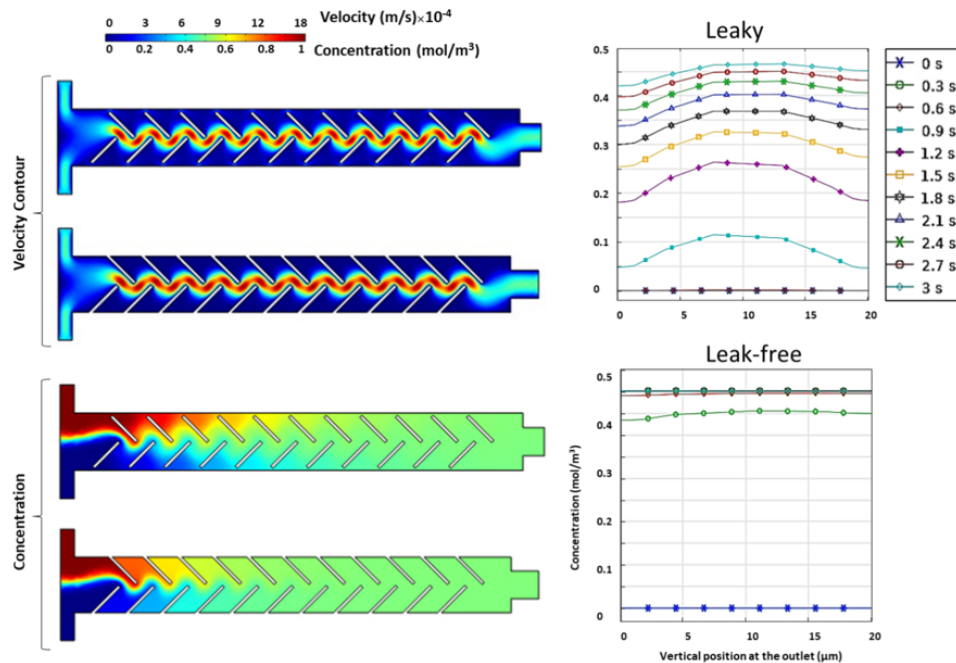


**Figure 7.** Velocity contour, concentration distribution, and concentration diagram at the outlet for the 45° micromixer with a double length of 380  $\mu\text{m}$

#### 4 Conclusion

This study investigated the impact of obstacles with varying angles in the flow path on the mixing performance of the micromixers. Two designs were compared: a leaky configuration and a leak-free configuration. The results demonstrated that the presence and orientation of obstacles exerted a significant influence on microscale mixing behavior. In all the angles studied in this study, the leak-free design demonstrated superior performance, achieving shorter mixing lengths and times, along with higher mixing efficiency. Specifically, in the leak-free design, mixing efficiency decreased as the angle of the obstacles increased. However, in the leaky design, changes in mixing efficiency did not correspond proportionally to variations in the angle of the obstacles. Both designs revealed that using obstacles inclined at 15° provided the most effective mixing enhancement. Additionally, simulation results specified that increasing the length of the mixing path considerably reduced mixing time and improved mixing quality in the leak-free configuration. Nonetheless, mixing time remained dependent on the geometry of the microchannel. Simulations offer a cost-effective means for investigating the impact of the various parameters on desired outcomes, making them a valuable tool for researchers. The design examined in this study is both simple and feasible to construct compared to other passive micromixer designs from previous research, while still exhibiting strong performance.

#### Data Availability

The data used to support the research findings are available from the corresponding author upon request.

#### Acknowledgments

Portions of this work were previously presented at the 21st Fluid Dynamics Conference, held in Bushehr, Iran, in 2025.

#### Conflicts of Interest

The author declares no conflicts of interest.

## References

- [1] X. Wang, Z. Liu, B. Wang, Y. Cai, and Q. Song, "An overview on state-of-art of micromixer designs, characteristics and applications," *Anal. Chim. Acta*, vol. 1279, p. 341685, 2023. <https://doi.org/10.1016/j.aca.2023.341685>
- [2] D. Soltani, T. Persoons, and S. Alimohammadi, "Micromixing strategies for efficient mixing processes: A comprehensive review," *J. Micromech. Microeng.*, vol. 34, no. 11, p. 113001, 2024. <https://doi.org/10.1088/1361-6439/ad809a>
- [3] W. Han, W. Li, and H. Zhang, "A comprehensive review on the fundamental principles, innovative designs, and multidisciplinary applications of micromixers," *Phys. Fluids*, vol. 36, no. 10, p. 101306, 2024. <https://doi.org/10.1063/5.0238393>
- [4] Y. Lu, W. Tan, S. Mu, and G. Zhu, "A multi-vortex micromixer based on the synergy of acoustics and inertia for nanoparticle synthesis," *Anal. Chim. Acta*, vol. 1239, p. 340742, 2023. <https://doi.org/10.1016/j.aca.2022.340742>
- [5] B. Liu, B. Ran, C. Chen, L. Shi, Y. Liu, H. Chen, and Y. Zhu, "A low-cost and high-performance 3D micromixer over a wide working range and its application for high-sensitivity biomarker detection," *React. Chem. Eng.*, vol. 7, no. 11, pp. 2334–2347, 2022. <https://doi.org/10.1039/D2RE00103A>
- [6] S. Zhu, Y. Fang, Y. Chen, P. Yu, Y. Han, N. Xiang, and Z. Ni, "Stackable micromixer with modular design for efficient mixing over wide Reynold numbers," *Int. J. Heat Mass Transfer*, vol. 183, p. 122129, 2022. <https://doi.org/10.1016/j.ijheatmasstransfer.2021.122129>
- [7] X. Chen, T. Tang, J. Zhai, A. Liang, X. Li, and X. Chen, "Bioinspired leaf-vein micromixer for a rapid and efficient synthesis of monodisperse ciprofloxacin lipid nanoparticles," *Langmuir*, vol. 41, no. 29, pp. 19 572–19 581, 2025. <https://doi.org/10.1021/acs.langmuir.5c02493>
- [8] S. Roy, R. Kumar, A. Acooli, S. Roy, A. Chatterjee, S. Chattaraj, J. Nayak, B. H. Jeon, A. Basu, S. Banerjee *et al.*, "Transforming nanomaterial synthesis through advanced microfluidic approaches: A review on accessing unrestricted possibilities," *J. Compos. Sci.*, vol. 8, no. 10, p. 386, 2024. <https://doi.org/10.3390/jcs8100386>
- [9] E. Chiesa, A. Caimi, M. Bellotti, A. Giglio, B. Conti, R. Dorati, F. Auricchio, and I. Genta, "Effect of micromixer design on lipid nanocarriers manufacturing for the delivery of proteins and nucleic acids," *Pharmaceutics*, vol. 16, no. 4, p. 507, 2024. <https://doi.org/10.3390/pharmaceutics16040507>
- [10] R. M. Camarillo-Escobedo, J. L. Flores, J. M. Camarillo-Escobedo, E. Hernandez-Campos, and L. H. Garcia-Muñoz, "Design and evaluation of micromixers fabricated with alternative technologies and materials for microanalytical applications in situ," *Chemosensors*, vol. 13, no. 5, p. 191, 2025. <https://doi.org/10.3390/chemosensors13050191>
- [11] M. A. A. Abdelhamid, M. R. Ki, H. J. Yoon, and S. P. Pack, "Microfluidic sensors for micropollutant detection in environmental matrices: Recent advances and prospects," *Biosensors*, vol. 15, no. 8, p. 474, 2025. <https://doi.org/10.3390/bios15080474>
- [12] M. Juraeva and D. J. Kang, "Design and analysis of a passive micromixer based on multiple passages," *Micromachines*, vol. 16, no. 5, p. 592, 2025. <https://doi.org/10.3390/mi16050592>
- [13] P. L. Ahl, "Microfluidic and turbulent mixing for mRNA LNP vaccines," *Pharmaceutics*, vol. 17, no. 9, p. 1148, 2025. <https://doi.org/10.3390/pharmaceutics17091148>
- [14] L. von Damnitz and D. Anders, "A review on the mixing quality of static mixers," *ChemEngineering*, vol. 9, no. 6, p. 128, 2025. <https://doi.org/10.3390/chemengineering9060128>
- [15] A. Ganguli, V. Bhatt, A. Yagodnitsyna, D. Pinjari, and A. Pandit, "A review of pressure drop and mixing characteristics in passive mixers involving miscible liquids," *Micromachines*, vol. 15, no. 6, p. 691, 2024. <https://doi.org/10.3390/mi15060691>
- [16] M. I. Pryazhnikov, A. V. Minakov, D. V. Guzei, A. I. Pryazhnikov, and A. S. Yakimov, "Flow regimes characteristics of water–crude oil in a rectangular Y-microchannel," *J. Appl. Comput. Mech.*, vol. 8, no. 2, pp. 655–670, 2022. <https://doi.org/10.22055/JACM.2021.38784.3282>
- [17] Z. Zhao, M. Su, J. Yuan, L. Yang, and X. Chen, "Optimal design of passive micromixers using the combination of computational fluid dynamics and machine learning," *J. Braz. Soc. Mech. Sci. Eng.*, vol. 47, p. 198, 2025. <https://doi.org/10.1007/s40430-025-05509-w>
- [18] S. R. Bazaz, A. Sayyah, A. H. Hazeri, R. Salomon, A. A. Mehrizi, and M. E. Warkiani, "Micromixer research trend of active and passive designs," *Chem. Eng. Sci.*, vol. 293, p. 120028, 2024. <https://doi.org/10.1016/j.ces.2024.120028>
- [19] A. Kheirkhah Barzoki, "Optimization of passive micromixers: Effects of pillar configuration and gaps on mixing efficiency," *Sci. Rep.*, vol. 14, p. 16245, 2024. <https://doi.org/10.1038/s41598-024-66664-z>
- [20] M. Wojnicki, X. Yang, P. Zabinski, and G. Mutschke, "Enhanced mixing in microflow systems using magnetic

- fields—Experimental and numerical analyses,” *Micromachines*, vol. 16, no. 4, p. 422, 2025. <https://doi.org/10.3390/mi16040422>
- [21] P. Majumdar and D. Dasgupta, “Enhancing micromixing using external electric and magnetic fields,” *Phys. Fluids*, vol. 36, no. 8, p. 082013, 2024. <https://doi.org/10.1063/5.0221764>
- [22] J. C. Hsu, “Enhanced micromixing using surface acoustic wave devices: Fundamentals, designs, and applications,” *Micromachines*, vol. 16, no. 6, p. 619, 2025. <https://doi.org/10.3390/mi16060619>
- [23] A. Husain, A. I. Khan, W. Raza, N. Al-Rawahi, N. Al-Azri, and A. Samad, “Design and mixing performance of passive micromixers: A critical review,” *J. Eng. Res.*, vol. 19, no. 2, pp. 106–128, 2023. <https://doi.org/10.53540/TJER.VOL19ISS2PP106-128>
- [24] N. Bikkinina, A. Bulatova, and O. Solnyshkina, “Impact of spatial configuration on fluid flow through a microchannel with fin pin array,” *J. Appl. Comput. Mech.*, vol. 12, no. 1, pp. 164–175, 2026. <https://doi.org/10.22055/jacm.2025.47994.4897>
- [25] M. Juraeva and D. J. Kang, “Design and mixing analysis of a passive micromixer with circulation promoters,” *Micromachines*, vol. 15, no. 7, p. 831, 2024. <https://doi.org/10.3390/mi15070831>
- [26] Y. Liao, Y. Mechulam, and B. Lassalle-Kaiser, “A millisecond passive micromixer with low flow rate, low sample consumption and easy fabrication,” *Sci. Rep.*, vol. 11, p. 20119, 2021. <https://doi.org/10.1038/s41598-021-99471-x>
- [27] Y. Zhang and X. Chen, “The mixing performance of passive micromixers with smart-rhombic units,” *J. Dispersion Sci. Technol.*, vol. 43, no. 3, pp. 439–445, 2022. <https://doi.org/10.1080/01932691.2020.1842759>
- [28] X. Chen and H. Lv, “New insights into the micromixer with Cantor fractal obstacles through genetic algorithm,” *Sci. Rep.*, vol. 12, p. 4162, 2022. <https://doi.org/10.1038/s41598-022-08144-w>
- [29] S. Cai, Y. Jin, Y. Lin, Y. He, P. Zhang, Z. Ge, and W. Yang, “Micromixing within microfluidic devices: Fundamentals, design, and fabrication,” *Biomicrofluidics*, vol. 17, no. 6, p. 061503, 2023. <https://doi.org/10.1063/5.0178396>
- [30] M. B. Okuducu and M. M. Aral, “Toward the next generation of passive micromixers: A novel 3-D design approach,” *Micromachines*, vol. 12, no. 4, p. 372, 2021. <https://doi.org/10.3390/mi12040372>
- [31] S. Akar, A. Taheri, R. Bazaz, E. Warkiani, and M. Shaegh, “Twisted architecture for enhancement of passive micromixing in a wide range of Reynolds numbers,” *Chem. Eng. Process. Process Intensif.*, vol. 160, p. 108251, 2021. <https://doi.org/10.1016/j.cep.2020.108251>
- [32] S. Jain and H. N. Unni, “Design and simulation of microfluidic passive mixer with geometric variation,” *Int. J. Res. Eng. Technol.*, vol. 5, no. 2, pp. 55–58, 2016. <https://doi.org/10.15623/ijret.2016.0502011>